Non-isotropic Omnidirectional Imaging System for an Autonomous Mobile Robot

Kazuaki Kondo and Yasushi Yagi
The Institute of Scientific and Industrial Research
Osaka University
Mihogaoka 8-1 Ibaragishi Osaka, Japan
kondo,yagi@am.sanken.osaka-u.ac.jp

Masahiko Yachida
Graduate School of Engineering Science
Osaka University
Machikaneyama 2-1 Toyonakashi Osaka, Japan
yachida@yachi-lab.sys.es.osaka-u.ac.jp

***Abstract*— A real-time omnidirectional imaging system that can acquire an omnidirectional field of view at video rate using a convex mirror was applied to a variety of conditions. The imaging system consists of an isotropic convex mirror and a camera pointing vertically toward the mirror with its optical axis aligned with the mirror's optical axis. Because of these optics, angular resolution is independent of the azimuth angle. However, it is important for a mobile robot to find and avoid obstacles in its path. We consider that angular resolution in the direction of the robot's moving needs higher resolution than that of its lateral view. In this paper, we propose a non-isotropic omnidirectional imaging system for navigating a mobile robot.**

***Index Terms*— Mobile Robot, Omnidirectional imaging system, Distribution of resolution, Discovering obstacles**

I. Introduction

Over the past 15 years, researchers in the fields of computer vision, applied optics and robotics have presented a number of papers related to omnidirectional cameras and their various applications. There have been several attempts to acquire omnidirectional images using a rotating camera [1], multi cameras [2], a fish-eye lens, and convex mirrors [3], [4], [5]. Omnidirectional cameras consisting of a CCD camera and a convex mirror placed in front of a camera which can simultaneously observe panoramic images, are used for robot navigation and problems related to human interaction.

For navigation, a robot's vision must generate a spatial map of its environment for path planning, obstacle collision avoidance, and finding candidates for interesting objects. For this, a detailed analysis is not necessary but high speed and a rough understanding of the environment around the robot is required. For instance, Omnidirectional observation gives robust ego-motion estimation [9], [10], [11] and can discover obstacles in any direction. Benosman proposed a special camera for map building; it can observe both sides of the robot by using a cylindrical hyperbolic mirror [13], but it can not observe over a 360 degree panoramic view. For a RoboCup soccer robot, Bonarini proposed a fast tracking method in a multiple mobile robots environment [7]. Nakamura proposed a special catadioptric sensor that can obtain an orthographic projection of the floor, without any software processing, for generating a 2D map [8]. Conroy proposed omnidirectional vision with constant latitude resolution to acquire uniform panoramic images in a latitudinal direction [6]. However, these sensors focus on special tasks.

Generally, tasks of an intelligent mobile robot can be classified into two categories; navigating to a goal, and operation at the goal. For object manipulation or detailed analysis of an interesting object, a limited field of view is sufficient but a high resolution is required (namely a local view). However, the resolution of an omnidirectional camera is not sufficient for this purpose, since an omnidirectional view is projected onto an image with limited resolution, say 512x480. A high-resolution frontal image is good for functions such as tele-operation, manipulation, and recognition.

The aim of our research project is to create a new omnidirectional camera for an intelligent mobile robot. The camera will need to satisfy multiple requirements for navigation and manipulation tasks. In this paper, we propose a new omnidirectional camera in which the distribution of the image resolution is continuously changed using an extended biconic paraboloidal mirror. This camera is suitable for navigation because it can simultaneously and continuously observe an omnidirectional view, and nearly useful enough omnidirectional image processing can be applied. A common omnidirectional camera has a constant but low angular resolution of the azimuth. Usually, a high resolution image is required for object recognition and precise manipulation. Thus, the image resolution of our proposed camera is approximately twice higher than that of a common omnidirectional camera at its front and rear views.

Since compactness and being light-weight are important design features of mobile robots, our research team has proposed a multiple image sensing system (MISS) on a single camera with two types of imaging; omnidirectional and binocular vision [12]. The concept of omnidirectional vision and local vision is similar; but in this the peripheral and central regions of the image plane are used for omnidirectional sensing and local vision, respectively. The basic idea of changing resolution is similar to ESCHeR [14] that simulated a human optical system. It is like a fish-eye lens system with 180 degree semi-spherical view (peripheral view). The central region of the image is a high resolution area that is like the center of a human retina.

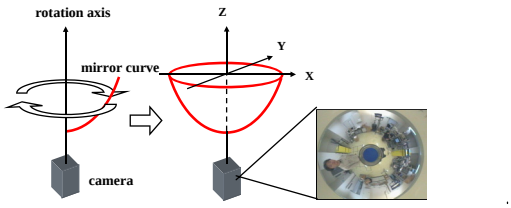

Fig. 1. Omnidirectional imaging so far developed consists of a vertical aiming camera and a rotational convex mirror; an example of an input image. The camera's optical axis is aligned to the mirror's rotational axis.

An advantage of this optical system is that tracking and focus of attention tasks are easy to change because both view fields are defined continuously. A disadvantage for navigation is that it can not observe a 360 degree panoramic view. We apply this concept of changing resolution to omnidirectional imaging for navigating an autonomous robot.

II. Non-isotropic Omnidirectional Camera

A. Designing an imaging system

Standard omnidirectional cameras with a convex mirror have isotropic properties. Because, the shape of a convex mirror is defined by rotating a curvature around the optical axis of the camera as shown in Fig. 1. For instance, all points with the same azimuth in space appear on a radial line through the image center, and its direction indicates the azimuth. Such conventional mirror imaging systems have constant resolution about the azimuth angle.

To change the resolution of an image by the observational direction, we propose a non-isotropic optic system. One simple idea is to stretch the mirror shape along a horizontal axis. A horizontal section of the mirror becomes an ellipse from a circle, and will have non-isotropic properties. The shape stretching also makes for an efficient use of the rectangular input image plane. However, this way of deformation has two problems. One concerns the observation of a horizontal section of the world. For a mobile robot, observation of a horizontal section of the world is very important in many of its applications (Fig. 2). In the case of isotropic imaging systems that use hyperboloidal, paraboloidal or spherical mirrors, the height of horizontal incident rays are independent of its azimuth angle. But in the case of a non-isotropic mirror, incident rays from the horizon do not have the same height for different mirror curvatures about the azimuth. The other problem concerns the distribution of spatial resolution. A simple stretched mirror has a reverse changing property between resolutions longitudinally and latitudinally, as shown in Fig. 3. This means nearly there is constant spatial resolution about the azimuth angle, which is not required. Therefore, we design a mirror that is able to obtain a horizontal section of the world in the following way. With simple stretching, focal points of mirror curvatures on radial sections go up and down only on the Z axis as the azimuth angle changes. We thus put respective focal points not only on the Z axis but also on the radial section plane to increase design

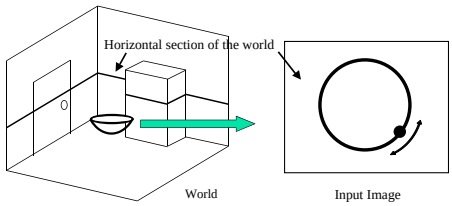

Fig. 2. Horizontal section of the world. Object on a horizontal section only moves on a given circle in the input image, when the robot moves in a 2D motion. This property shows the importance of acquiring the horizontal section image for mobile robot navigation.

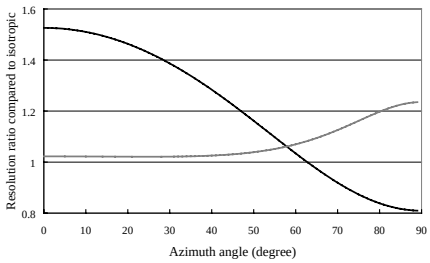

Fig. 3. Example of resolution distribution with simple stretching of the mirror as a ratio to isotropic resolution (An anamorfic lens can create this property).

freedom(Fig. 4). At the same time, the previous distribution of spatial resolution problem is solved by this focal point shifting (details are explained later. refer Fig. 7).

In this paper, we propose a concept of non-isotropic omnidirectional imaging based on a paraboloidal mirror using "simple stretching" and "focal point shifts" ideas. Omnidirectional imaging based on a parabolic curvature and "focul point shifts" is generally represented by the following equations.

$$\begin{cases} X = t\cos\theta \\ Y = t\sin\theta \\ Z = At^2 + Bt + C \end{cases} \qquad \begin{cases} x = X \\ y = Y \end{cases} \tag{1}$$

where A, B, C are parabolic coefficients. t, θ are polar description of XY plane. Left set of equations shows mirror shape, and right one shows projection from mirror XYZ onto an image plane xy, which is orthogonal

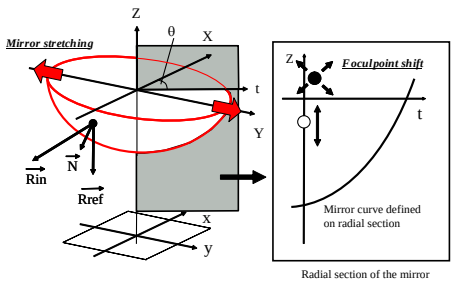

Fig. 4. Geometry of the proposed non-isotropic mirror system. Mirror stretching along the Y axis gives its horizontal section ellipse, which delivers a non-isotropic property to resolution distribution. Focal points are fixed on the Z axis with only mirror stretching, but at any position on a radial section of the mirror with our non-isotropic concept.

projection. We apply "simple stretching" and a "horizontal section of the world" condition to Eq. (1) for acquiring a non-isotropic property.

(Condition 1: Simple stretching condition)

$$\frac{X^2}{a^2} + \frac{Y^2}{b^2} = 1 \quad at \quad Z = 0 \tag{2}$$

(Condition 2: Horizontal section of the world)

$$\overrightarrow{R_{in}} = \overrightarrow{R_{ref}} - 2\frac{\overrightarrow{N} \cdot \overrightarrow{R_{ref}}}{|\overrightarrow{N}|^2} \cdot \overrightarrow{N} \tag{3}$$

$$\overrightarrow{N} = \begin{bmatrix} cos\theta \\ sin\theta \\ \frac{\partial Z}{\partial t}|_{Z=0} \end{bmatrix} \times \begin{bmatrix} 1 \\ \frac{\partial Y}{\partial X}|_{Z=0} \\ 0 \end{bmatrix} \tag{4}$$

where a and b are elliptic coefficients deciding shape of horizontal section of the mirror at Z=0, which makes how amount of non-isotropic property the mirror has. $\overrightarrow{R_{in}}, \overrightarrow{R_{ref}}, \overrightarrow{N}$ are vectors of incident and reflected rays and the mirror normal, respectively. $\overrightarrow{R_{ref}} = [0, 0, -1]^t$ for orthogonal camera projection. To acquire a horizontal section of the scene, the condition that the z term of $\overrightarrow{R_{in}}$ =0 at Z=0 is needed.

We finally get a non-isotropic omnidirectional imaging system expressed by the following equation. We named this imaging system the Horizontal fixed viewpoint Biconic (HBP) mirror system.

$$\begin{cases} X = t\cos\theta \\ Y = t\sin\theta \\ Z = \frac{2D(\theta)-a}{2L(\theta)^2}t^2 - \frac{D(\theta)-a}{L(\theta)}t - \frac{a}{2} \\ L(\theta) = ab\sqrt{\frac{\tan^2\theta+1}{a^2\tan^2\theta+b^2}} \\ D(\theta) = ab\sqrt{\frac{a^2\tan^2\theta+b^2}{a^4\tan^2\theta+b^4}} \end{cases} \quad \begin{cases} x = X \\ y = Y \end{cases} \tag{5}$$

B. prototype HBP mirror system

We made a prototype HBP mirror system based on Eq. (5). The design coefficients are a=34mm, b=42mm. It is difficult as well as being not realistic to make up a 68mm by 84mm orthogonal projection; so we use a parabolic mirror to translate the orthogonal projection to a perspective projection for a normal perspective camera. You can use a smaller HBP mirror and a telecentric lens to avoid two-mirror construction, as an another way to satisfy orthogonal projection. Fig. 5 and Fig. 6 show an overview of a prototype HBP mirror system and examples of input images, respectively. We put a 50mm by 50mm checker pattern at a distance of 400mm. The optical properties, such as blur and aberration, are sufficient for practical use. A vertical straight line in a view of the world is projected as a little curved radial line in the input images, but it can be dealt with as a straight line in a local area. We can also apply a navigation method based on vertical edge detection[15] in the scene to the HBP mirror system. Resolution changing through simulation and experimental results with the prototype HBP mirror about the azimuth angle are shown in Fig. 7 In the proposed HBP mirror,

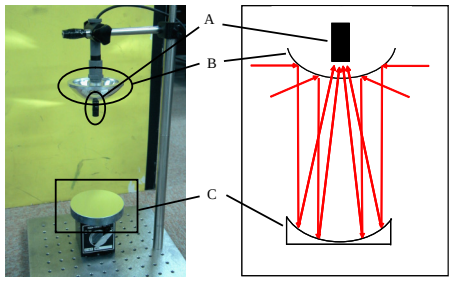

Fig. 5. Overview of prototype HBP mirror system. (Left) real overview. (Right) ray trace model of the HBP mirror system. (A) Normal perspective camera. (B) HBP mirror. (C) parabolic mirror. Incident rays from a scene are reflected by the HBP mirror and become parallel, and are reflected again by the parabolic mirror to concentrate on the perspective camera focus.

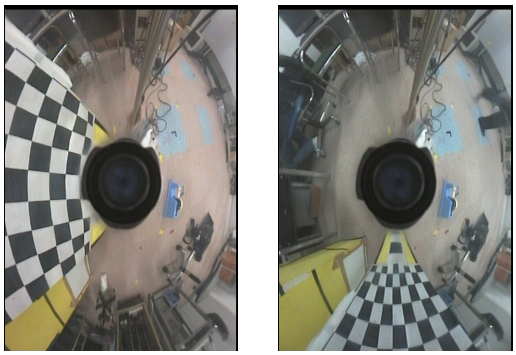

Fig. 6. Example of input images with HBP mirror. (Left) putting the checker board on the short radius side (aligned to the robot's path). (Right) long radius side. We can see that the checkers on the short radius side are bigger than on the long radius side.

both longitunal and latitunal resolutions are higher near $0degree(moving-direction)$ than near $90degree(side-direction)$. A HBP mirror has worse resolution than an isotropic near $90degree$, but observation in this direction is not important for a mobile robot. We describe how this lower resolution influence is used to discover obstacles in Section III-B. Different from a simple stretched mirror, a HBP mirror has spatial resolution bias about the azimuth angle, because the latitunal resolution changes as well as the longitunal. Logitunal resolution plots with the prototype HBP mirror in Fig. 7 approximately fall in a range of digital error band, which shows same resolution property in simulation. We retain the properties effective for robots; omnidirectional images, real time processing, observation of a horizontal section and of a vertical line projected as a radial one, Also, the HBP mirror system has spatial resolution bias about the azimuth angle.

III. Experiment of Obstacle Detection and Time-to-Collision Estimation

By aligning the high resolution direction of the HBP mirror to a robot's moving path, the robot can discover obstacles approaching earlier. In this section, we evaluate and compare the ability of discovering obstacles through experiments. In simulation, we use $a = 35mm, b = 50mm$ and $a = b = 35mm$ as designing coefficients for

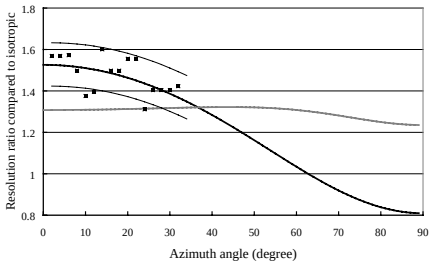

Fig. 7. Resolution distribution with a HBP mirror (a=34mm, b=42mm) as a ratio to isotropic resolution. Black line and gray line show longitunal resolution and latitunal resolution, respectively. Experimental results are shown by plots and digital error band occuring from CCD element size is described by thin lines.

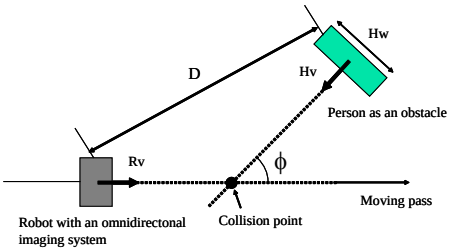

Fig. 8. Collision between an omnidirectional imaging system mounted on a mobile robot and an approaching object. $R_v = 80cm/sec, H_v = 150cm/sec, H_w = 70cm$ considering a general indoor room environment. ϕ is the collision angle, and D the obstacle detection distance; a longer D means an earlier detection.

the HBP mirror and the isotropic mirror for comparison, respectively; and use the prototype HBP mirror noted in Section II-A for a real experiment.

The collision model including parameters such as velocity and length used in the experiments is shown in Fig. 8. We decided the coefficients of the HBP mirror system (mobile robot) and an obstacle object (human) considering a general indoor environment. The observation frame rate is 10 Hz for real time control of the mobile robot.

A. Frontal crash detection using optical flow expansion

Optical flow is defined as a point moving between two different frame images, and is used for many tasks with mobile robots. For example; ego motion, depth estimation, and obstacle detection. Because an object approaching towards an imaging system causes an expansion of the optical flow, finding and estimating the center point of the expansion of the optical flow leads to the detection of approaching objects. However, to detect the optical flow expansion point, which often appears near the moving path of a robot, is difficult due to its small size. So we designed a HBP mirror having high resolution in the forward and backward directions to achieve a longer optical flow and to accurately detect the point.

$\phi = 0$ in Fig. 8 describes the situation where objects approach from in front of the robot and causes a frontal crash. Fig. 9 showing the optical flow size relative to the distance between the robot and the moving object as an obstacle, demonstrates the applicability of the HBP mirror

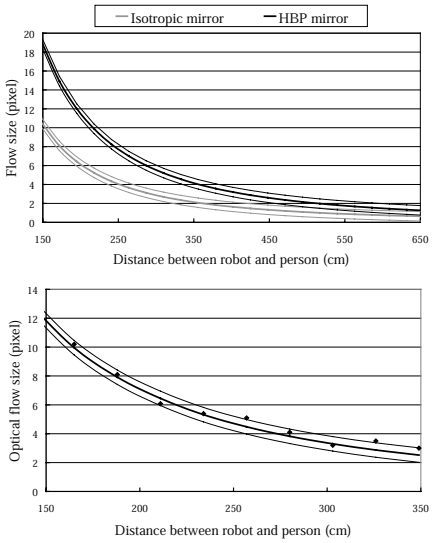

Fig. 9. Optical flow size of an object approaching from a forward angle $\phi = 0$. (Upper) the results of the simulation. (Bottom) the results of the prototype HBP mirror. In both figures, the thick line is the ideal value, thin lines are the digital error band, and the plots are real values.

in this frontal crash case. For example when the distance between them is 360cm, the flow size of the HBP mirror (4 pixels) is twice as big as that of an isotropic mirror (2 pixels), which means more accurate detection. Further, assume that a 2 pixel flow provides obstacle detection, a robot can detect over a distance of 450cm-580cm with a HBP mirror in contrast to 320cm-410cm with an isotropic mirror, which provides earlier detection. The prototype HBP mirror system had the above optical flow sensibility.

B. Omnidirectional collision

Omnidirectional imaging can detect not only frontal obstacles but also obstacles in any direction, and can thus move about more safely. We assumed a size of 2 pixels as the obstacle detection threshold of the optical flow; to estimate the distance between the imaging system and approaching objects relative to $-\pi < \phi < \pi$. The results of the mirror stretching ratio candidates $K = \frac{b}{a} = 1.4(a = 35mm, b = 50mm), 1.8, 3.0$, are shown in Fig. 10, comparing each surrounding length constant with each other. Using a HBP mirror, earlier detection can be realized not only on moving paths but also in the neighborhood of $\phi = 0, \pi$. With $K = 1.4$, the HBP mirror, because of the longer distance in range of $-\frac{\pi}{2} < \phi < \frac{\phi}{2}$, the obstacle detection ability of the HBP mirror is available for avoiding frontal crashes, bumps from behind, collisions at cross roads before they occur, all situation that often occur in daily life in places like an office building. With $K = 1.8, 3.0$, a HBP mirror is more capable of detecting frontal and behind crashes at the cost of its side detection ability, so these HBP mirrors are suitable for long and thin environments like a in pipe or a duct. Resolution lowering at the orthogonal orient of the moving path allows detection at shorter distances near $\phi = \frac{3}{4}\pi$. But this is an obstacle that acts like pulling over to a kerb. We consider

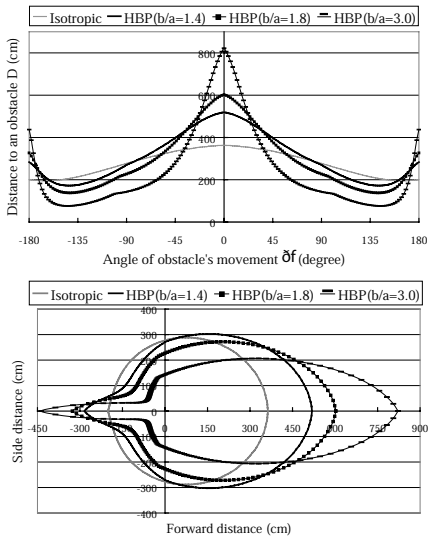

Fig. 10. Obstacle detection distance D relative to collision angle ϕ. (Upper) orthographic presence. (Bottom) polar presence. The lateral axis represents the moving path of the robot (right direction is forward).

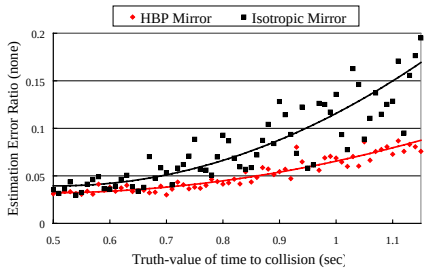

Fig. 11. Results of time-to-collision estimation. Plots are experimental results and block lines are fitting curvature. In all ranges of time-distance, the HBP mirror can estimate time-to-collision accurately because of its lower error average and variance.

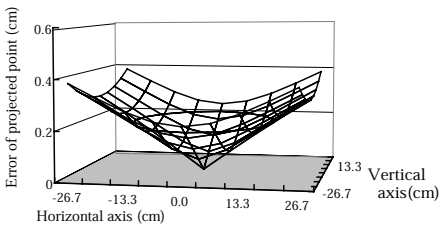

Fig. 12. Misalignment of the projection point. The bottom plane is the projected image spread, and the vertical axis is the misalignment error. Error does not appear on the X and Y axes, and increases with distance from these axes. We think that a $0.4cm$ error relative to an image spread of about $55cm$ can be ignored.

that the lessened detection in the above situation is not a problem, as such cases are rare in the assumed operational environment.

C. Estimation of time-to-collision

In the most cases, after detecting obstacles approaching it, a robot plans an avoidance path based on the distance to the obstacle. As images only have azimuth information and don't have depth information, it is impossible to know the distance without known lengths (for example such as the stereo method, where a basic line between two cameras is known). However, we can estimate distance as TIME, which does not include length information, called time-to-collision. Time-to-collision can be estimated by using optical flows; its accuracy depends on the correctness of the calculated optical flows. Our HBP mirror has high resolution and can acquire accurate optical flows, which gives it a high accuracy in estimations of time-to-collision.

Fig. 11 describes the estimation error of time-to-collision with the conditions used in Section III-A. Though Tistarell proposed a time-to-collision estimate method [16], they used optical flow as a continuous function, and this is not suitable for digital control of a robot. So we estimate the time-to-collision assuming that the target object has uniform motion relative to the robot during the period of three frames - two continuous optical flows. Lowering both error average and variance in Fig. 11shows that the HBP mirror has more accurate and stable estimation of time-to-collision.

IV. Multi-viewpoint problem

At the same time as it is navigating, an autonomous robot must undertake operational tasks such as manipulation and recognition. Detailed images in front of the robot are available for tele-operation, or presentation. Our proposal of the HBP mirror system also fulfills these requirements. Usually, omnidirectional input images are projected into other coordinate systems such as perspective, orthographic, polar or cylindrical for image processing. Because a 2D image does not having depth information, the depth of the projection screen is decided as a constant value by the user or programmer. Omnidirectional cameras proposed in the past had single viewpoints that all incident rays cross at a single point, this is a perspective system. So the geometry between the object and projected image is conserved, other than for the scale factor, independent of the depth of an object. On the other hand, a HBP mirror which breaks the single viewpoint property to achieve resolution bias has a number of viewpoints. In a multi-viewpoint system, the above geometry is not conserved; each point is not projected at the correct position. We compare object and projected images, then evaluate the influence of point's misalignment in the following two experiments. The isotropic and HBP mirrors in these experiments are the same ones as used in Section III.

A. Absolute amount of misalignment

The causes of misalignment are dependent on the object's and the project screen's depths. By way of example, Fig. 12 shows the distance between a projected point and the correct point in front of the robot, when the depth of the object $D_o = 150cm$ and the project screen $D_s = 100cm$. We consider that a $0.4cm$ misalignment to an object of about $55cm$ in size is very small, and can be ignored (this value is smaller than the CCD resolution, as the case maybe).

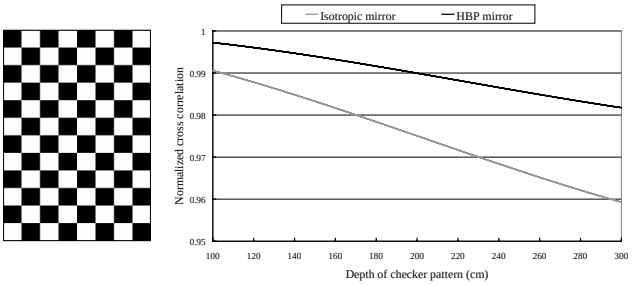

Fig. 13. (Left) template checker pattern used in the experiment. (Right) normalized cross correlation between projected checker image and the template checker. Though the object depth $100cm$ is equal to the projected screen depth, correlation is not 1. This is why a misalignment does not appear in this case, but a reduction of resolution causes a lowering of the correlation.

B. Influence to correlation

It is more important for recognition that the projected image is similar to the real object rather than that there is less partial misalignment. We estimate this image similarity by calculating the cross correlation between the two images, using the checker images as an object. Normalized cross correlation between the projected checker image and the template checker image is shown in Fig. 13, when the projected screen depth is $D_s = 100cm$, the object checker image depth changes, $D_o = 100cm - 300cm$. A HBP mirror has a higher correlation than an isotropic one at all object depths, in contrast to our expectation that the HBP mirror would have lesser correlation than an isotropic one. That is why both misalignment and also image resolution have effects on image correlation. In other words, the fusion of the point misalignment and the high resolution influence result in a high correlation with the HBP mirror. As it is necessary for correlation to normalize image size of a templete image and an input image, low resolution images with the isotropic mirror have bigger influence of aliasing(image expansion) or information luck(image reduction), we consider. In the details of Fig. 13, the HBP and isotropic mirrors have almost the same correlation value near the camera, for misalignment has as much effect as resolution. Distant from the camera, because of the scaling down of the recognition target in the input image, misalignment rarely appears and resolution has much influence on correlation. Thus, the proposed HBP mirror maintains a relatively high correlation for long distances. Results using our prototype HBP mirror and a toy doll as an object, as shown in Fig. 14, also demonstrate similar correlation properties.

V. CONCLUSIONS

In this paper, we proposed a non-isotropic omnidirectional imaging system that we named the HBP mirror; the mirror has high resolution in the direction of its moving path. In the experimental results, the HBP mirror system retains a lot of the properties that the isotropic mirrors have, and the system was shown to be suitable for many tasks an autonomous mobile robot must undertake, such as

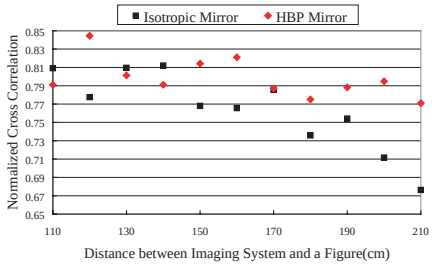

Fig. 14. Normalized cross correlation with using the prototype HBP mirror and a 20cm by 22cm toy doll.

obstacle detection or object recognition. Though the multi-viewpoint causes distorted projection, the amount of this is very small, and high resolutions can allow for accurate recognition objects over reasonable distances.

REFERENCES

[1] J. Y. Zheng and S. Tuji, "Panoramic Representation of Scenes for Route Understanding", Proc. IEEE Int. Conf. Robotics and Automation, pp. 161-167, 1990.
[2] T. Kawanishi, K. Yamazawa, H. Iwasa, H. Takemura, and N. Yokoya, "Generation of high-resolution stereo panoramic images by omnidirectional imaging sensor using hexagonal pyramidal mirrors", Proc. Int. Conf. Pattern Recognition, pp. 485-489, 1998.
[3] Y. Yagi and S. Kawato, "Panorama scene analysis with conic projection", Proc. IEEE/RSJ Int. Workshop on Intelligent Robotics and Systems, pp. 181-187, 1990.
[4] Shree K. Nayer, "Catadioptic Omnidirectional Camera", in Proc. of CVPR, pp. 482-488, 1997.
[5] K. Yamazawa, Y. Yagi, M. Yachida, "Visual Navigation with Omnidirectional Image Sensor HyperOmni Vision", in IEICE Vol.J79 No. 5, pp. 698-707, May 1996.
[6] T. L. Conroy and J. B. Moore, "Resolution Invariant Surfaces for Panoramic Vision Systems", Proc. IEEE Int. Conf. Computer Vision, Vol. 1, pp. 392-397, 1999.
[7] A. Bonarini, P. Aliverti, M. Lucioni, "Omnidirectional Vision System for Fast Tracking for Mobile Robots", IEEE Trans. Instrumentation and Measurement, Vol. 49, No. 3, pp. 509-512, 2000.
[8] T. Nakamura and H. Ishigro, "Automatic 2D Map COnstruction using a Special Catadioptric Sensor", Proc. IEEE/RSJ Int. Conf. Intelligent Robotics and Systems, pp. 196-201, October 2002.
[9] Joshua Gluckman, Shree K. Nayer, "Ego-motion and Omnidirectional Cameras", in Proc. of ICCV, pp. 999-1005, 1998.
[10] Iren Stratmann, "Omnidirectional Imaging and Optic Flow", in Proc. of IEEE Workshop on OMNIVIS, pp. 104-111, 2002.
[11] Raqual Frizera Vassallo, Jose Santos-Victor, Hans Jorg Schneebeli, "General Approach for Egomotion Estimation with Omnidirectional Images", in Proc. of IEEE Workshop on OMNIVIS, pp. 97-103, 2002.
[12] Y. Yagi, H. Okumura and M. Yachida, "Multiple visual sensing system for mobile robot", Proc. IEEE Int. Conf. Robotics and Automation, vol. 2, pp. 1679-1684.
[13] R. Benosman, E. Deforas, J. Devars, "A New Catadioptric Sensor for the Panoramic Vision of Mobile Robots", in Proc. of IEEE Workshop on OMNIVIS, pp. 112-118, 2000.
[14] Y. Kuniyoshi, N. Kita, K. Sugimoto, S. Nakamura and T. Suehiro, "A foveated wide angle lenses for active vision", Proc. IEEE Int. Conf. Robotics and Automation, pp. 2982-2988, 1995.
[15] Y. Yagi, K. Shouya, M. Yachida, "Environmental map generation and ego-motion estimation in a dynamic environment for an omnidirectional image sensor", Proc. IEEE Int. Conf. Robotics and Automation, pp. 3493-3498, 2000.
[16] M. Tistarelli, G. Snadini, "Direct Estimation of Time-to-impact from Optic Flow", in Proc. of IEEE1991 Workshop on Visual Motion, pp. 226-233, 1991.